Journal of Power Sources 271 (2014) 65–75

Contents lists available at ScienceDirect

Journal of Power Sources

journal homepage: www.elsevier.com/locate/jpowsour

Morphology control of zinc regeneration for zinc–air fuel cell and battery

Keliang Wang, Pucheng Pei*, Ze Ma, Huachi Xu, Pengcheng Li, Xizhong Wang

State Key Lab. of Automotive Safety and Energy, Tsinghua University, Beijing 100084, China

HIGHLIGHTS

- Solutions to morphology control of zinc regeneration.
- Effect of variables on morphological evolution analyzed by COMSOL.
- Discussing mechanism of morphological change by Monte Carlo method.
- Microstructures of deposited zinc were examined by way of SEM.

ARTICLE INFO

Article history:
Received 25 June 2014
Received in revised form
26 July 2014
Accepted 28 July 2014
Available online 6 August 2014

Keywords:
Zinc regeneration
Morphology control
Zinc–air fuel cell/battery
Simulating methods

ABSTRACT

Morphology control is crucial both for zinc–air batteries and for zinc–air fuel cells during zinc regeneration. Zinc dendrite should be avoided in zinc–air batteries and zinc pellets are yearned to be formed for zinc–air fuel cells. This paper is mainly to analyze the mechanism of shape change and to control the zinc morphology during charge. A numerical three-dimensional model for zinc regeneration is established with COMSOL software on the basis of ionic transport theory and electrode reaction electrochemistry, and some experiments of zinc regeneration are carried out. The deposition process is qualitatively analyzed by the kinetics Monte Carlo method to study the morphological change from the electrocrystallization point of view. Morphological evolution of deposited zinc under different conditions of direct currents and pulse currents is also investigated by simulation. The simulation shows that parametric variables of the flowing electrolyte, the surface roughness and the structure of the electrode, the charging current and mode affect morphological evolution. The uniform morphology of deposited zinc is attained at low current, pulsating current or hydrodynamic electrolyte, and granular morphology is obtained by means of an electrode of discrete columnar structure in combination with high current and flowing electrolyte.

1. Introduction

Appropriate energy storage plays a more important role in a wide range of applications, including frequency regulation of renewable energy sources, peak-shaving of electrical grid, emergency power and portable power [1,2]. Metal-air batteries have received much attention due to their high energy densities [3], where oxygen from the air employed as their cathode material. Compared with other metals, zinc possesses a variety of advantages: low equilibrium potential, high specific energy, good environmental compatibility, good reversibility, it is found in abundance and it is easy to handle [4]; therefore, zinc material is widely applied to the electrochemistry field in either the galvanization or in cathode active material [5,6]. However, several major problems in zinc regeneration need to be addressed including zinc pellets of appropriate size, shape change of zinc electrode and dendritic growth [7]. These are particularly important for zinc–air battery due to seriously affecting the battery's durability and performance, limiting the applications of the zinc–air secondary battery. Moreover, zinc–air fuel cells' performance is subject to zinc pellets size, because it can determine active surface area, and influence electrolyte flowing and contact resistance.

Although such morphological changes arise from ionic transport through diffusion, migration and convection, the mechanism for causing morphological changes remains unknown. Some researchers have made significant progress in exploring the

* Corresponding author. Tel./fax: +86 10 62788558.
E-mail address: pchpei@mail.tsinghua.edu.cn (P. Pei).

http://dx.doi.org/10.1016/j.jpowsour.2014.07.182
0378-7753/

mechanism for the morphological changes of zinc electrodes [8–10]. McBreen [11] developed a concentration-cell model that accounted for the shape change of zinc electrodes during charge/discharge, but for slow or fast diffusion further explanation are needed. Choi et al. [12,13] proposed a hydrodynamic model for shape change based on electrolyte flows in a battery as a consequence of osmotic and electro-osmotic forces which explains the ionic movement from the zinc electrode's top toward its bottom, but this method cannot provide reasonable explanations for the zinc accumulation at the center of the electrode. Bockris et al. held that dendritic growth might be closely related to the overpotential at the tip of the dendrites [8]. They also investigated the relationship between the dendritic formation and the physical properties of an electrolyte such as composition, temperature, viscosity, and hydrodynamics [14]. In addition, some researchers have done some work in solutions to zinc dendrites. Parker et al. [15] designed a porous electrode to suppress growth of zinc dendrites. Smedley et al. [16] provided a solution of zinc regeneration with optimizing the structure of zinc electrode to control zinc morphology. Shaigan et al. [17] employed pulsating current as morphological control of electrodeposited zinc. Other researchers have also made some attempt to model the zinc electrode. Deiss et al. [18] developed a one-dimensional numerical model of an electrically rechargeable alkaline zinc–air battery that can predict decrease of the zinc redistribution with increasing cycle number. Song et al. [19] established a one-dimensional mathematical model of the discharge process and of the failure mechanisms of zinc electrode, predicting variable distributions within the electrode itself. Bauer et al. [20] put forward a model of the numerical simulation of copper electrodeposition. Braff et al. [21,22] established a two-dimensional model for simulating a hydrogen bromine laminar flow fuel cell based on COMSOL software. To control the morphological change, the mechanism for shape change must be further studied, and then put forward reasonable solutions.

In this work, we investigated the morphological change of zinc electrode related to parametric conditions with COMSOL software, and experiments on zinc electrodeposition under the conditions of different current and flowing electrode were also conducted. Furthermore, we implemented zinc depositing process simulation relying on the three-dimensional kinetics Monte Carlo method, analyzing morphological evolution.

2. Experiment methods and numerical model

2.1. Experiment methods

An experimental apparatus for zinc electrodeposition was fabricated, where the cathode employed stainless steel, the anode used nickel network with the same dimension as the cathode, and the electrolyte was made of weight 40% potassium hydroxyl mixed with zinc oxide. The distance between the anode and the cathode is 5 mm, and the effective dimension of the cathode is about 30 mm × 30 mm. Zinc electrodeposition experiments were carried out at the room temperature, where the power supply with pulsating and galvanostatic mode was EA-PS 8065-10, and data acquisition instrument used for recording current signals was NI-PXI-1033. In addition, auxiliary components were not described here including a pump used for the flowing electrolyte. The morphology of deposited zinc was examined by scanning electron microscopy (JSM-6460). For some reason, hydrodynamic conditions, charging mode, and electrode structure can influence morphological change of electrodeposited zinc. Table 1 lists the different testing parameters including flowing electrolyte, charging mode and structure.

Table 1
Testing parameters for zinc electrodeposition.

Parameters	Feature I	Feature II
Electrode structure	Planar electrode	Porous electrode
Electrolyte state	Quiescent	Hydrodynamic
Charging mode	Direct current	Pulsating current

2.2. Numerical model

2.2.1. Electrode kinetics

Zinc electrodeposition involves energy conversion transforming electrical energy into chemical storage energy, accompanied by phase changes. Fig. 1 shows that chemistry and electrochemistry reactions occur near or on the electrodes of a zinc–air rechargeable battery during charge, where the morphological change of zinc regeneration is a concern because it reduces the capacity of the battery. Pulsating currents from new clean energy is more beneficial to suppress dendritic growth.

Zinc oxide or zincate is reduced at the cathode, and hydroxyl is oxidized at the anode during charge. The electrochemical reactions can be expressed as:

$$\text{Anode}: \quad 2OH^- \rightarrow \frac{1}{2}O_2\uparrow + H_2O + 2e \tag{1}$$

$$\text{Cathode}: \quad \begin{aligned} &ZnO + H_2O + 2OH^- \rightarrow Zn(OH)_4{}^{2-} \\ &Zn(OH)_4{}^{2-} + 2e \rightarrow Zn + 4OH^- \end{aligned} \tag{2}$$

The required charge voltage can be determined by the thermodynamic equilibrium voltages and the activation overpotentials at the anode and cathode, and ohmic loss of the electrolyte. Thus.

$$\Delta\varphi = E^a_{eq} - E^c_{eq} + \eta_a + \eta_c + iR_{el} \tag{3}$$

Butler–Volmer equations are used to describe the electrode reaction kinetics.

$$i_{loc} = i_0\left[\exp\left(\frac{\alpha_a F\eta}{RT}\right) - \exp\left(\frac{-\alpha_c F\eta}{RT}\right)\right] \tag{4}$$

where i_{loc} denotes the local current density at the solid–liquid interface, i_0 exchange current density, α_a anodic transfer coefficient, α_c cathodic transfer coefficient, F/RT the Nernst factor, and η activation overpotential for the electrode reactions, which can be defined as the below equation:

$$\eta = \phi_s - \phi_l - E_{eq} \tag{5}$$

where ϕ_s is electrode potential, and ϕ_l is electrolyte potential. According to the Nernst equation, equilibrium potentials E_{eq} are calculated by:

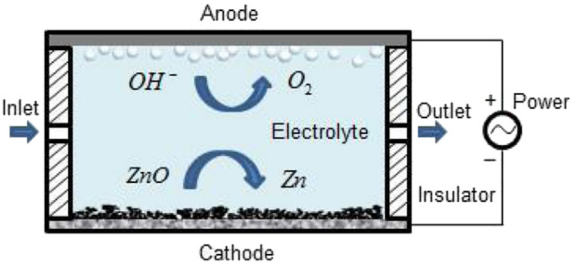

Fig. 1. Schematic view of zinc electrodeposition.

$$E_{eq}\left(Zn^{2+}/Zn\right) = E^0\left(Zn^{2+}/Zn\right) - \frac{RT}{2F}\ln\frac{c_{Zn}}{c_{Zn^{2+}}}$$
$$E_{eq}\left(OH^-/O_2\right) = E^0\left(OH^-/O_2\right) - \frac{RT}{2F}\ln\frac{[c_{O_2}]^{\frac{1}{2}}}{[c_{OH^-}]^2} \quad (6)$$

The potential drop in the electrolyte is also part of the charging voltage, which depends on the ionic current, electrolyte concentration, and conductivity. An empirical relation can be described by:

$$i = -\sigma\nabla\phi_l \quad (7)$$

where σ is the electrolyte conductivity, and ϕ_l is the potential in the electrolyte.

2.2.2. Species transport

Transport of ions in the electrolyte is controlled by diffusion, migration, and convection. Diffusion stems from concentration difference, migration is determined by additional power, and convection comes from fluid dynamics. The material balance equation can be expressed as:

$$\frac{\partial c_k}{\partial t} + v\cdot\nabla c_k - \nabla\cdot(D_k\nabla c_k + z_k\mu_k F c_k\nabla\phi_l) = R_{k,s} \quad (8)$$

where c_k stands for the species concentration, v the fluid velocity, D_k the diffusion coefficient, z_k the charge for ionic species, μ_k the mobility of the charged species, subscript k designates species (i.e. $Zn(OH)_4^{2-}$, OH^-, K^+), F Faraday's constant, and $R_{k,s}$ is reaction rate.

The model of electrolyte movement employs incompressible Navier–Stokes equation as follows.

$$\rho\left(\frac{\partial v}{\partial t} + v\cdot\nabla v\right) = -\nabla p + \mu\nabla^2 v + f \quad (9)$$

The electroneutrality condition is also taken into account.

$$\sum_{k=1}^{n} z_k\cdot c_k = 0 \quad (10)$$

The electrode boundaries will move during zinc deposition. The molar flux of zinc N_{Zn} (mol $(m^2\ s)^{-1}$) over the electrode can be described by Faraday's law according to:

$$N_{Zn} = -\frac{\nu_{Zn} i_{loc}}{nF} \quad (11)$$

where the stoichiometric coefficients for zinc is $\nu_{Zn} = 1$ for both the electrode reactions, and the number of electrons is $n = 2$.

The depositing velocity v_{dep} (m s^{-1}) directed in the normal direction of the electrode into the electrode domain, can be deduced from the molar flux, the density and the molar mass of zinc.

$$v_{dep} = \frac{M_{Zn} N_{Zn}}{\rho_{Zn}} \quad (12)$$

2.2.3. Boundary conditions

In this work, zinc electrodeposition model was constructed using COMSOL Multiphysics software and kinetics Monte Carlo method. To simplify the model, we assume that the electrolyte flow with laminar and similarity technique is applied to surface roughness of the cathode. Different flowing velocities, different charging modes, and different surface morphology of the electrode were investigated on the basis of the model.

A schematically three-dimensional model for the zinc electrodeposition is shown in Fig. 2, which contains four governing equations, four field variables, and nine boundary conditions. We make the assumption that species concentration of the electrolyte is well-distributed at the flowing direction and the rest parts are insulated in addition to the electrolyte and the electrodes. Table 2 lists the relevant variables and expressions in the simulation process. Therein the electrolyte conductivity is assumed to be constant due to the flowing electrolyte counteracting concentration change during electrodeposition.

3. Results and discussion

3.1. Zinc regeneration process

Zinc electrodeposited process includes three steps, namely ionic transport, electrochemical reaction and electrocrystallization, involving mass transfer, charge transfer, and zinc adatoms incorporated into metal lattice. The depositing morphology at the surface of the cathode is mainly controlled by reaction kinetics, diffusion, atomic bond, crystal nucleation, and crystal growth in space and time. The morphology of electrodeposited zinc is the balance result of thermodynamics and kinetics, as illustrated in Fig. 3, thereby bringing about three different growth modes including the Volmer–Welmer (VW) mode, the Frankvan-der-Merwe (FM) mode, and the Stranski–Krastanov (SK) mode [23]. Zinc atoms uniformly grow at the horizontal direction controlled by diffusion along the depositing surface, while mass transfer between atomic layers controlled by Eheilich–Schwoebel barrier (E_S) determine the uniformity at the vertical direction. The final morphology depends on the competition between the vertical growth and the horizontal growth of crystal planes.

Non-uniform morphology of deposited zinc may be induced by crystal imperfections such as point defects, edge and screw dislocations and crystal clusters [7]. Fig. 4 shows several depositing types of adatoms and islands on the substrate at the initial stage and the shape change of deposited zinc at the later stage from the atomic perspective. The morphological evolution of electrodeposited zinc may be simulated by means of kinetics Monte Carlo method [24], where zinc atom number at each depositing layer is unequal and decreases progressively due to energy disparity of zinc atoms by van der Waals' force and different overpotentials at different positions, resulting in morphological change.

The morphology of deposited zinc can be in the form of spongy, dendritic, boulder-like, layer-like, mossy, and filamentous [7], mostly depending on two-phase interface conditions and external charging mode. Zinc dendritic growth controlled by diffusion is one of morphological change, which can be described by the method of diffusion-limited aggregation [25]. Accordingly, many researchers described dendritic morphology and characteristics in metal electrodeposition on basis of fractal theory [26,27]. Layer-like structure arises from epitaxial growth along with crystal structure and orientation. Boulder-like deposit is known as isoprobability growth at different crystal faces and orientations. Mossy deposit is controlled by activation. These morphologies are closely linked to electrode structure, electrolyte hydrodynamics, and charging mode.

3.2. Structure optimization

Zinc electrode is essential in zinc regeneration either for zinc–air batteries or zinc–air fuel cells [28], where zinc electrode structure as a substrate of deposited zinc influences morphological evolution.

Zinc depositing surface was assumed to be comparatively uniform, not considering surface roughness of zinc electrode such as the planar electrode. Morphological changes of deposited zinc

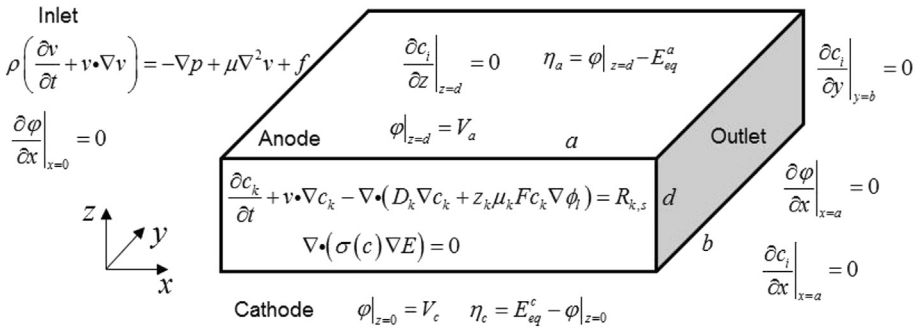

Fig. 2. Three-dimensional model for electrodeposited zinc.

Table 2
Variables and equations.

Quantity	Variable	Equation
Position	(x, y, z)	$L = a$ (m), $W = b$ (m), $H = d$ (m)
Electrolyte velocity	v	$v = Q/bd$ (m s^{-1})
Peclet number	Pe	Pe $= dv/D$
Flux density	φ	$\varphi = RT/F$ (V)

occur at the zinc electrode surface during charge, as shown in Fig. 5(a), where more zinc is deposited at the cathode edges than at the cathode center, but an alternative presents the preferable result by means of downsizing the cathode and smoothing the edges of the cathode (Fig. 5(b)). This phenomenon may be attributed to edge effect of the zinc electrode, leading to polarization easily at the periphery of the electrode. Therefore, the cathode and the anode should be kept parallel in structure, and the dimension of the anode is larger than that of the cathode, among which the cathode edges need to be round off.

Increasing surface roughness of zinc electrode like a porous electrode will cause morphological change, where the morphology of deposited zinc would be uneven over the surface of electrode at the early depositing stage, namely the more zinc deposited at the bulges, the less at the scallops. Fig. 6 shows local current densities distributed on the rough surface of the cathode, where the local current densities is higher at the bulges than at the scallops. Consequently, different surface microstructures lead to different current densities at the different points of the electrode, and then induce different deposit velocities. Besides, the porous electrode with high active area is available for diffusion of depositing atoms.

When an electrode of discrete columnar structure is employed as the cathode, the morphology of deposited zinc tends to be granular analogous to the column dimension. Fig. 7 shows the morphology of deposited zinc at the direct current density of 100 mA cm^{-2}, where the depositing mass change at the edges are higher than at the centers due to edge effects of electric field. It is even more important that zinc atoms only deposit, diffuse and aggregate on the small electrode surface, thus strengthening cohesion force among zinc atoms.

The gas bubbles produced by electrochemical reaction play a predominant role in the depositing morphology as well. Zinc–air battery was placed as the vertical position, leading to aggregation of oxygen bubbles at the upper electrolyte and driving the depositing atoms flowing towards downside during charge process, as shown in Fig. 8(a). Zinc–air battery was placed as the horizontal position, timely removing oxygen bubbles produced by reduction reaction, and the compact and uniform deposit layer was attained in Fig. 8(b).

3.3. Electrolyte management

Zincate concentration in the electrolyte affects the depositing morphology as well. Zincate concentration gradient will be formed between the bulk electrolyte and the interfacial electrolyte near the cathode as a result of electrochemical reaction, and zincate concentrations at different reaction zones will be different due to different reaction rates. For the purpose of uniformly stable species concentration of solution, it is necessary to make the electrolyte flow.

Assuming that the electrolyte move by way of laminar flow, the electrolyte between two parallel electrodes flows from one side towards the other side, with the middle part of the flowing velocity is higher than top and bottom parts. Now that convection induced by electrolyte hydrodynamics would hold dominant in species transport in the electrolyte relative to diffusion, there is a need to take full account of ions transport, electrolyte concentration and

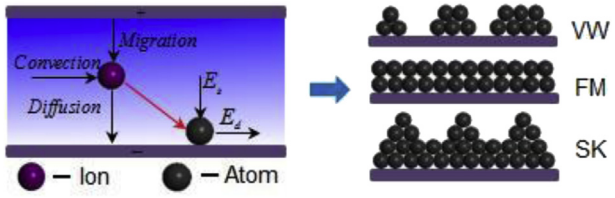

Fig. 3. Growth mode of electrodeposited zinc.

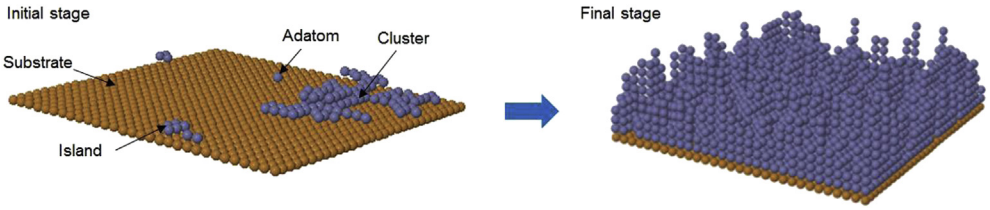

Fig. 4. Schematic process of electrodeposited zinc.

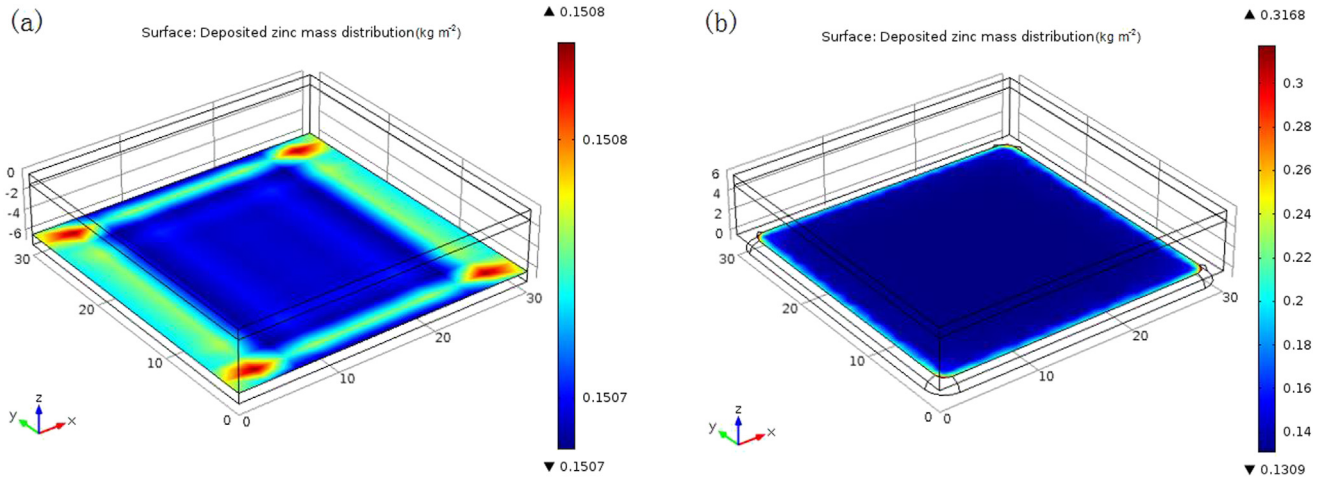

Fig. 5. Mass distribution of deposited zinc of parallel electrodes with different structures.

dendritic growth to optimize the flowing field. The flowing velocity of electrolyte can affect the distribution of species concentration and the morphology of zinc deposition. The larger the velocity, the more uniform the concentration, as shown in Fig. 9. However, the high velocity will scour nearby layer of deposited zinc owing to the small binding force among atoms on the sediment surface, and then cause shape change.

Fig. 10 shows that two different zinc depositing morphologies are obtained under the conditions of the quiescent electrolyte and the flowing electrolyte. Dendrites did not appear mainly because of convective flow of the electrolyte reducing concentration gradients between bulk electrolyte and surface electrolyte near the cathode, and taking away depositing atoms around dendrites. It is proved that the flowing electrolyte is an effective method to solve the problem of dendritic growth. However, the flowing electrolyte also washes away zinc deposits near the ingress and aggregated on other sites.

The flowing electrolyte can promptly take away gas bubbles avoiding gas aggregation near the anode. However, the high flowing velocity will adversely affect species transport, thus affect local current density of zinc electrode. Fig. 11 shows the local current density for the four Peclet numbers. The higher flow velocity for the

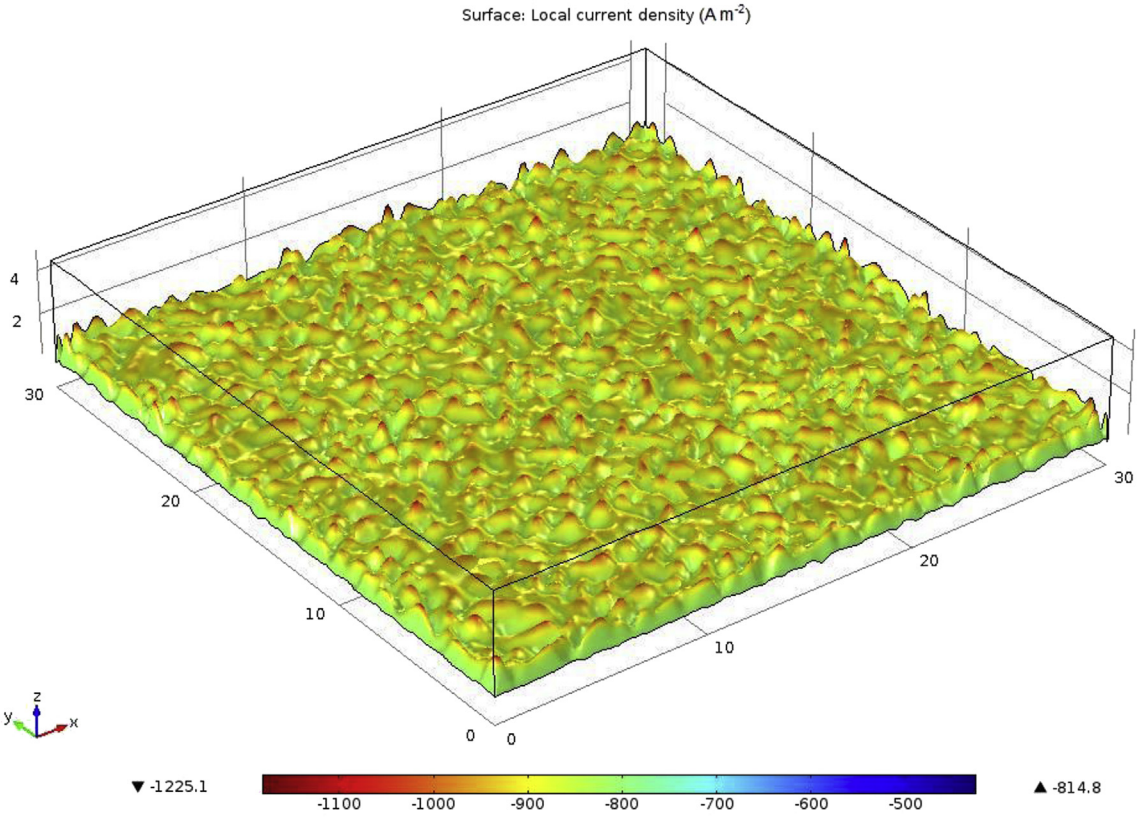

Fig. 6. Local current densities on the coarse surface of zinc electrode.

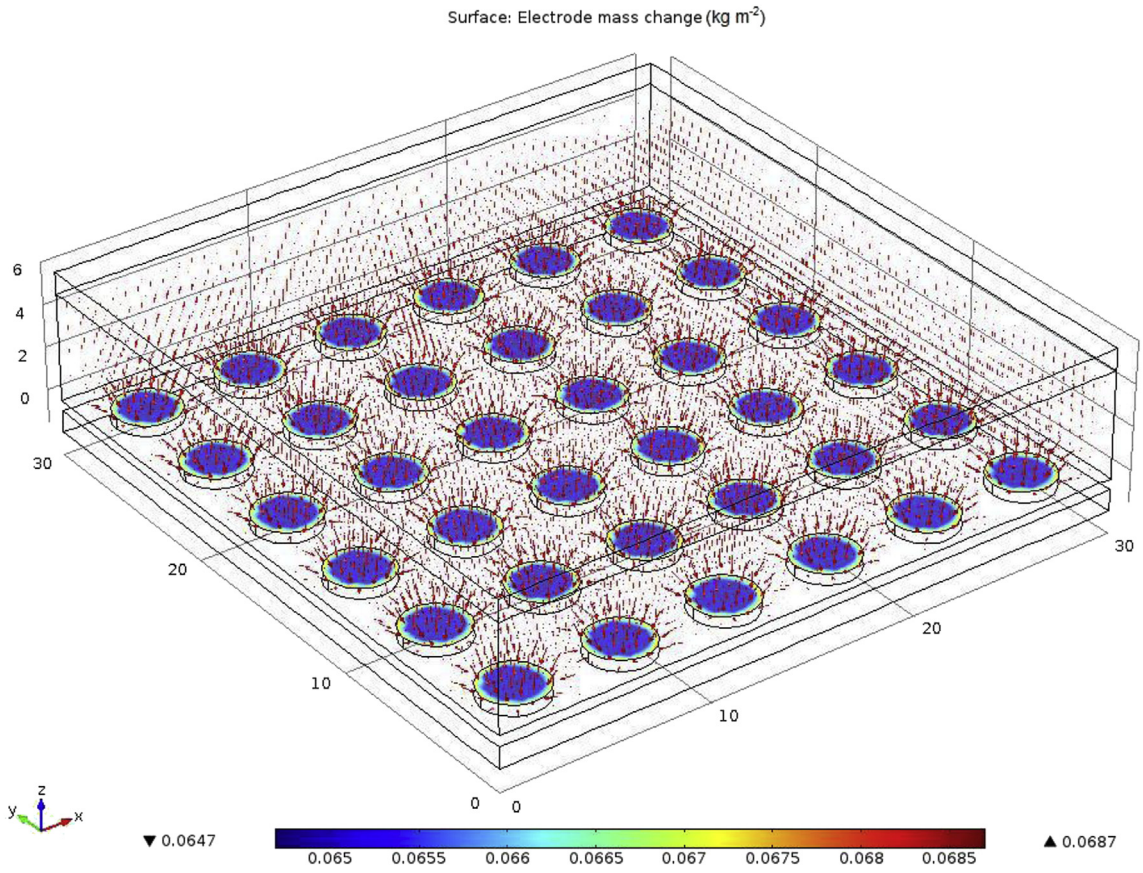

Fig. 7. Deposited zinc morphology on the discrete pins of electrode.

higher Peclet number will increase the local current density significantly due to the increased transport velocity of zinc ions.

It is found in Fig. 12 that maximum thickness of deposited zinc decrease under the condition of different fluid velocities, where increased flow rate cannot limit dendrites growth at small flowing velocities, properly because of this flow rate ameliorating concentration polarization between bulk electrolyte and reaction zone and improving local current densities on the cathode surface. However, zinc deposited thickness decreases with increased flow rate, attributed to driving force of hydrodynamic electrolyte exceeding bonding energy among zinc atoms.

In view of the above mentioned, it is found that the flowing electrolyte not only mitigates the instability of electrolyte characteristics during electrodeposition, but electrolyte hydrodynamics helps to improve ion diffusion and suppress zinc dendritic growth and take away gas bubbles in the zinc–air battery with alkaline electrolyte.

3.4. Charging mode

It is well-known that an increase in charging current accelerates the rate of ion migration, increases the number of activated ions, and enhances atom energy. Activation-controlled deposition plays a leading role at low current densities due to ions translating into atoms overcoming the activation energy barrier, while diffusion-controlled deposition dominates at high current densities. Fig. 13 shows that depositing morphology is the same as boulder-like at high current density, while compact at low current density.

Fig. 14 shows the trend of maximum deposited zinc thickness at different charging current densities of 100 A m^{-2}–2000 A m^{-2} at

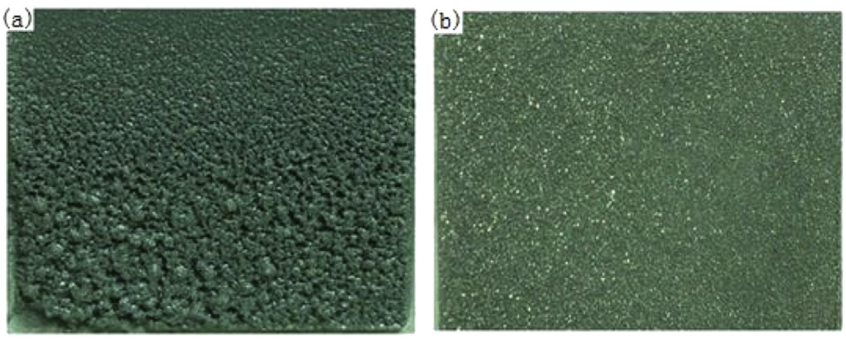

Fig. 8. Deposited zinc morphology in weight 40% KOH with saturated zinc oxide for 10 min at the current density of 100 mA cm^{-2}: (a) vertical position, (b) horizontal position.

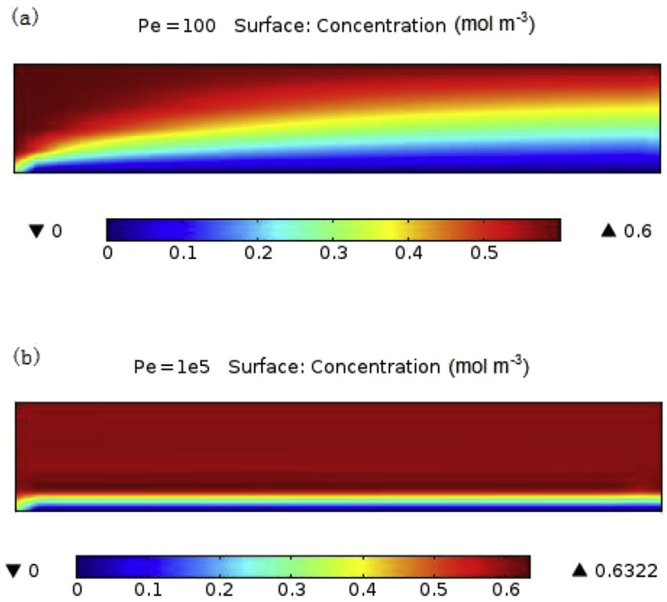

Fig. 9. Electrolyte concentration: (a) Pe = 100, and (b) Pe = 1e5.

the electric quantity of 3600 A s. The thickness of deposited zinc displays as a positive relationship with charging current mainly due to more electric quantity for zinc ions, therein the overpotential of zinc oxide reduction reaction increases towards minus direction resulting from polarization, and the voltage between the anode and the cathode increases with current densities. Zinc atoms will quickly diffuse and grow on the electrode surface at high current densities, leading to shorting and failure of zinc–air batteries. Meanwhile much more electrons may be wasted for hydrogen formation or non-Faradic reaction. This means that zinc regeneration in zinc–air battery need to take long time with small charging current, thus zinc morphological control at high charging currents is crucial for zinc–air batteries in application of energy storage.

Phase changes occur next to the electrodes during electrodeposition, including liquid–solid phase change and liquid–gas phase change. The production of hydrogen is companied by zinc electrodeposition which depends on electrolyte and electrode composition, charge mode, and temperature. Hydrogen bubbles can give birth to electrolyte convection, and thus affect zinc redistribution over the electrode. It is worth noting that gas bubbles may stay within depositing layer, and then lead to shape change especially for planar electrode, as shown in Fig. 15. To reduce hydrogen evolution, it is required to add a few inorganic elements or organic compounds into the electrolyte to increase the hydrogen evolution overpotential [29,30].

In addition, growth of dendrites is mainly controlled by diffusion at high current densities. Pulsating current or periodic reverse current deposition is conducive to improve the depositing morphology due to zincate ions having enough diffusion time. Fig. 16 displays that distinct results in morphology and depositing mass were obtained under conditions of direct current and pulsating current, respectively. It is found that the depositing morphology of zinc is greatly affected by the charging mode with duty cycle which is defined as $T_{on}/(T_{on} + T_{off})$. Reducing the duty cycle effectively improve the morphology of deposited zinc, namely compact morphology at the macrostructure scale and layer-like morphology at the micrometer scale attained under the condition of pulsating currents. Therefore, appropriate charging mode is an effective method to suppressing the dendritic growth.

Pulsating currents can improve the morphology of deposited zinc, namely pulse current with different duty cycles. Maximum

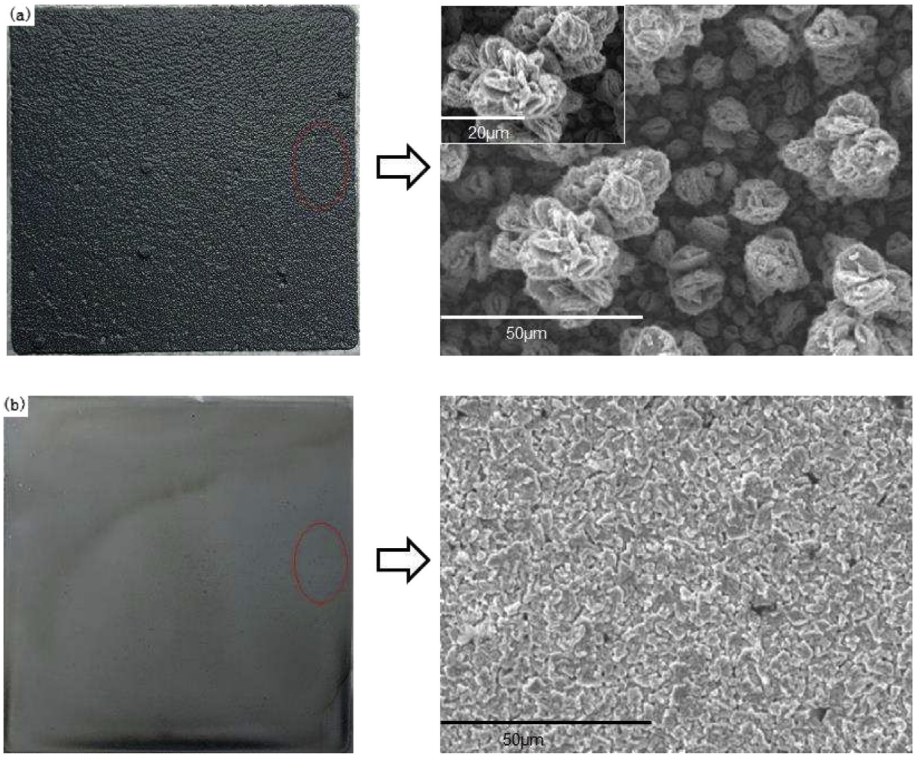

Fig. 10. Deposited zinc morphologies in weight 40% KOH with 1 M zinc oxide with electric quantity for 10 min at the current density of 100 mA cm^{-2}, (a) quiescent electrolyte, (b) flowing electrolyte.

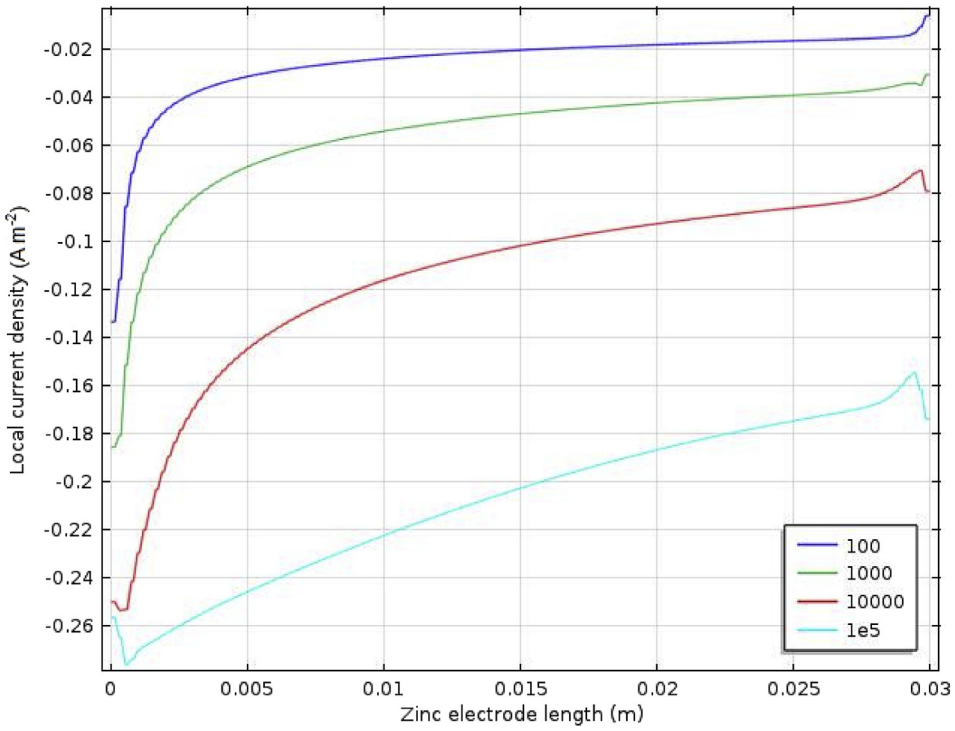

Fig. 11. Local current densities on the electrode surface for different Peclet numbers.

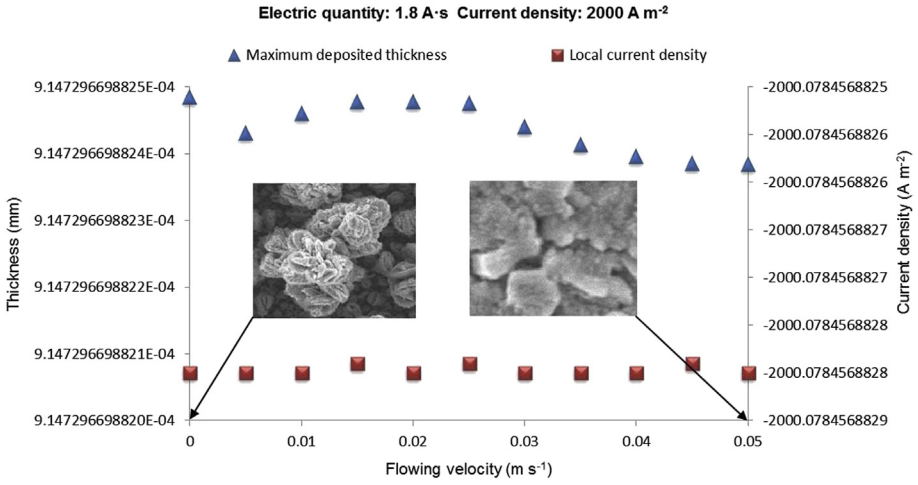

Fig. 12. Morphological evolution of deposited zinc at different flowing velocities of the electrolyte.

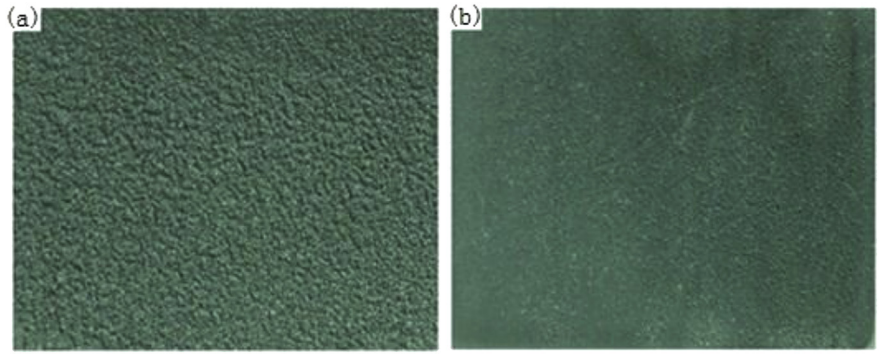

Fig. 13. Zinc depositing morphology in weight 40% KOH with saturated zinc oxide for 10 min under vertically positioned condition: (a) 50 mA cm^{-2} of current density, (b) 20 mA cm^{-2} of current density.

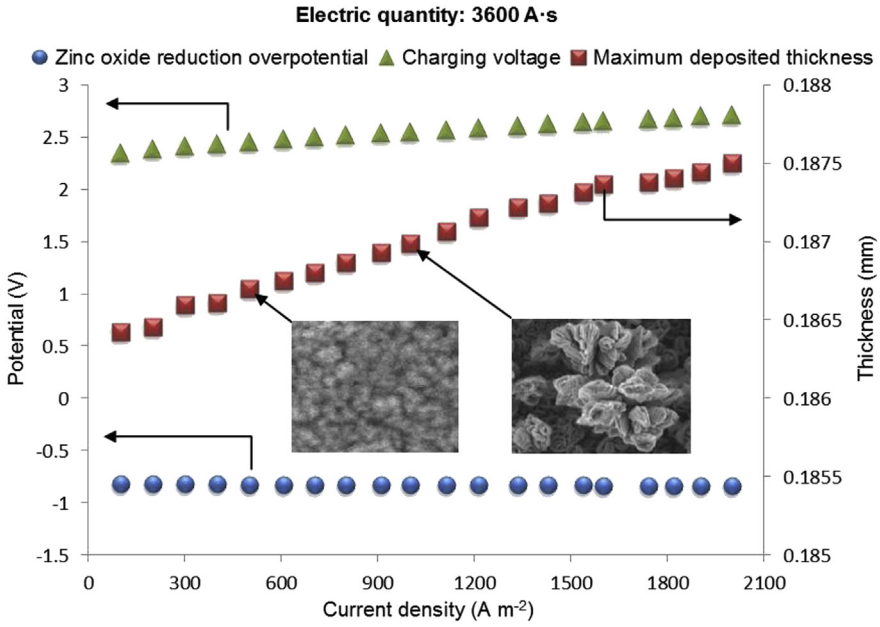

Fig. 14. Morphological evolution of deposited zinc at different charging currents.

thickness of deposited zinc tends to decrease with duty cycle reduction at the electric quantity of 16.2 A s in Fig. 17, as a result of diffusion of zinc atoms for off-time cycle. Therefore, morphological evolution is under control by means of charging mode, where high current combined with pulsating mode or small direct current is available for uniform morphology of deposited zinc.

Based upon the above results, we can see that shape change of zinc morphology on the cathode is closely related to local current densities under the same external conditions. However, dendritic growth may be effectively controlled by variables such as flowing electrolyte or pulsating current. Additionally, oxygen or hydrogen bubbles not only directly influence the depositing morphology, and deteriorate zinc–air battery's performance.

4. Conclusion

The mechanism for the morphological change of zinc electrodeposition in a zinc–air battery was investigated by means of three-dimensional kinetic Monte Carlo method and COMSOL software. The morphologies of deposited zinc under various testing conditions were also studied by way of scanning electron microscopy. The results show that the morphological change of deposited zinc mainly depends on local current densities of the cathode and are closely linked to working conditions as well, including the hydrodynamic electrolyte, charging mode, surface quality of the electrode, and structure. The detail is as follows:

1) Zinc morphology development depends on the rates of ion transfer, charge transfer and atom attachment at different depositing conditions, stemming from the factors of diffusion, activation and electrocrystallization. Different deposited morphologies are caused by different determining factors, among which dendritic growth is mainly controlled by diffusion.
2) Zinc deposited morphology control, where low current densities, duty cycle of pulsating currents and flowing electrolyte are in favor of mass and charge diffusion as well as high zincate

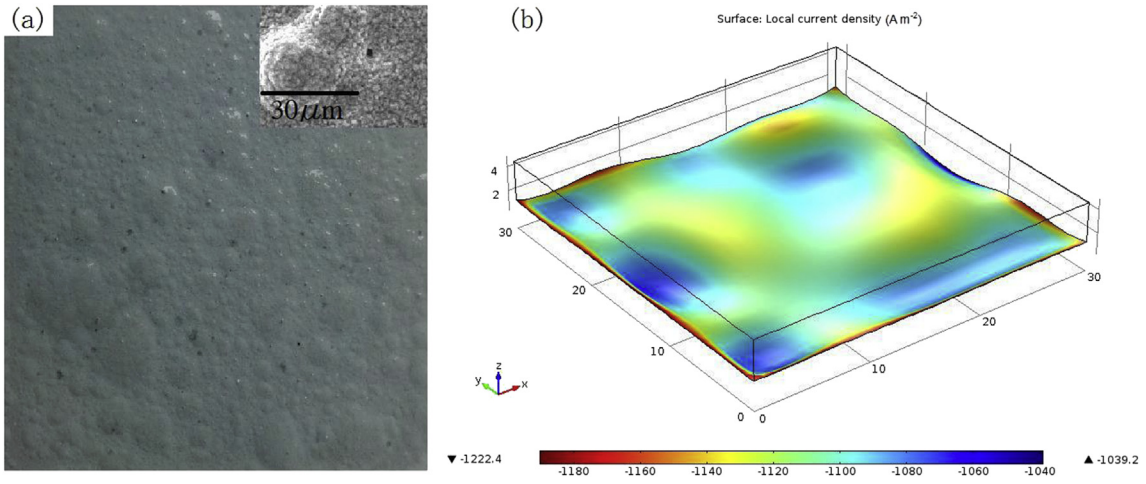

Fig. 15. (a) Zinc depositing morphology at 50 mA cm^{-2} of current density, (b) distribution of local current densities.

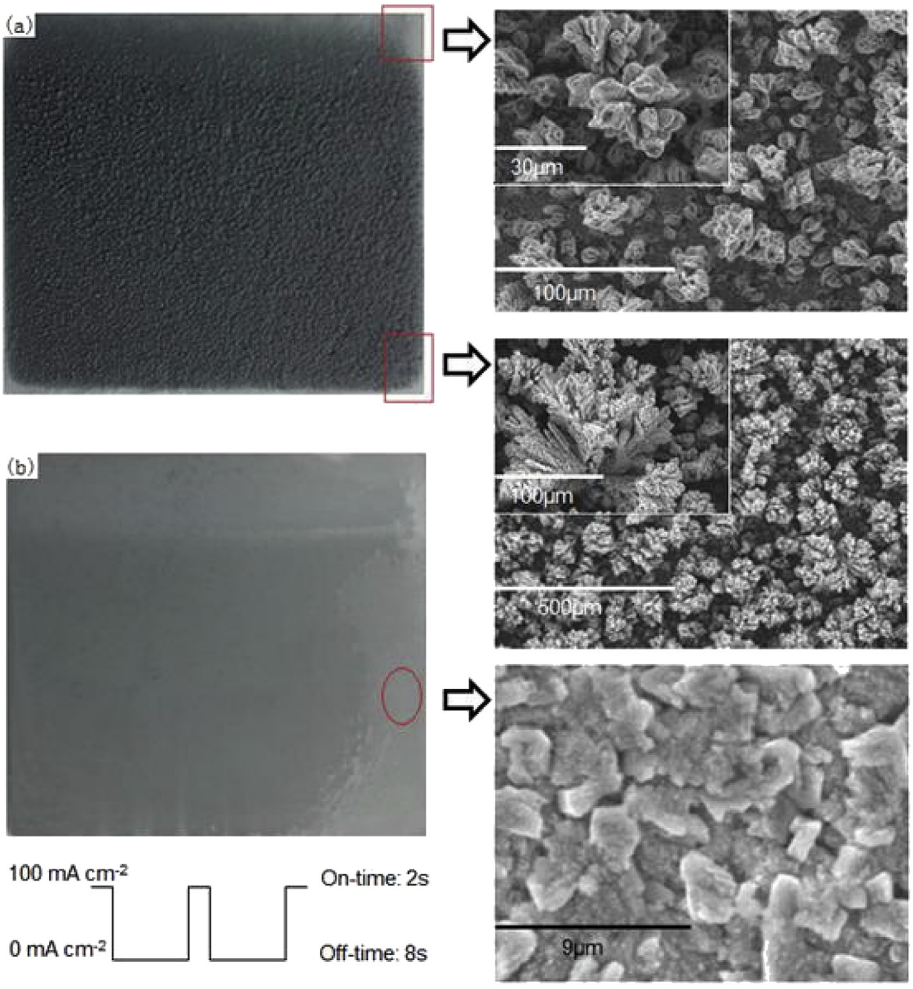

Fig. 16. Zinc depositing morphology with electric quantity for 10 min: (a) 100 mA cm^{-2} of direct current density, (b) 100 mA cm^{-2} of pulsating current density, 20% duty cycle.

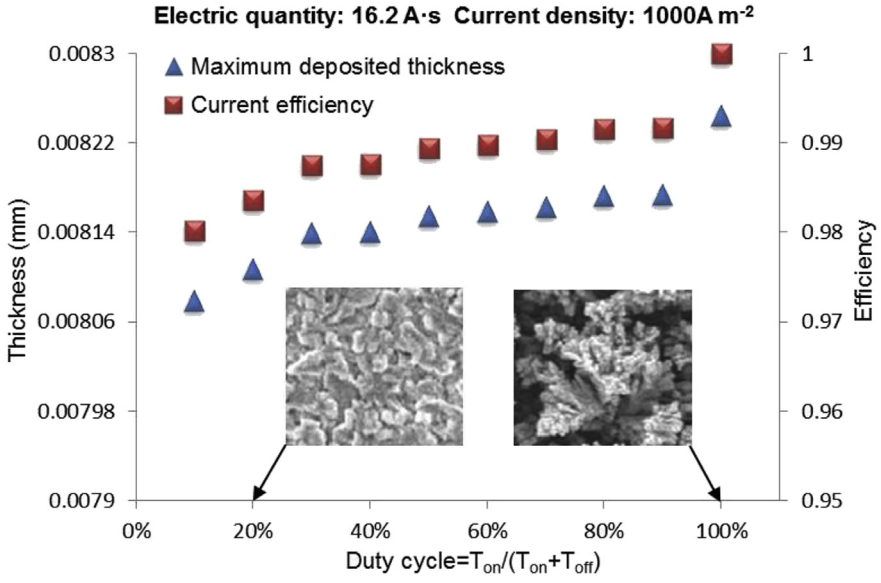

Fig. 17. Morphological evolution of deposited zinc at different duty cycles.

concentration and low KOH concentration, thus resulting in compact morphology of deposited zinc.

3) Even distribution of deposited zinc on the cathode surface, where horizontal layout of electrodeposited device is a preferred design for evenly distributed zinc deposition relative to vertical layout. In addition, electrolyte hydrodynamics and edge effect of zinc electrode also cause uneven distribution of deposited zinc.
4) Phase changes of zinc, hydrogen and oxygen during charge, where these phase changes influence morphological evolution and distribution. Hydrogen evolution can cause convective electrolyte to increase charge transfer rate, resulting in randomly nucleation, and oxygen aggregation will separate the anode from the electrolyte, leading to reduction of current efficiency.

Acknowledgments

This work has been funded by National Natural Science Foundation of China (21376138), National Basic Research Program of China (973 Program) (2012CB215505), and National High Technology Research and Development Program of China (863 Programs) (2012AA1106012, and 2012AA053402).

References

[1] J. Rugolo, M.J. Aziz, Energy Environ. Sci. 5 (5) (2012) 7151–7160.
[2] G.L. Soloveichik, Annu. Rev. Chem. Biomol. Eng. 2 (2011) 503–527.
[3] J.S. Lee, T.K. Sun, R. Cao, N. Choi, M. Liu, K. Lee, J. Cho, Adv. Energy Mater. 1 (1) (2011) 34–50.
[4] G.X. Zhang, ECS Trans. 16 (34) (2009) 47–59.
[5] B. Dunn, H. Kamath, J. Tarascon, Science 334 (6058) (2011) 928–935.
[6] F.R. McLarnon, E.J. Cairns, J. Electrochem. Soc. 138 (2) (1991) 645–656.
[7] R.Y. Wang, (Ph.D. thesis), University of Toronto, 2006.
[8] J.W. Diggle, A.R. Despic, J. Bockris, J. Electrochem. Soc. 116 (11) (1969) 1503–1514.
[9] R.D. Naybour, J. Electrochem. Soc. 116 (4) (1969) 520–524.
[10] K.I. Popov, M.D. Maksimović, J.D. Trnjančev, M.G. Pavlović, J. Appl. Electrochem. 11 (2) (1981) 239–246.
[11] J. McBreen, J. Electrochem. Soc. 119 (12) (1972) 1620–1628.
[12] K.W. Choi, D.N. Bennion, J. Newman, J. Electrochem. Soc. 123 (11) (1976) 1616–1627.
[13] K.W. Choi, D. Hamby, D.N. Bennion, J. Newman, J. Electrochem. Soc. 123 (11) (1976) 1628–1637.
[14] J.L. Barton, J. Bockris, Ser. A. Math. Phys. Sci. 268 (1335) (1962) 485–505.
[15] J.F. Parker, C.N. Chervin, E.S. Nelson, D.R. Rolison, J.W. Long, Energy Environ. Sci. 7 (2014) 1117–1124.
[16] S.I. Smedley, X.G. Zhang, J. Power Sources 165 (2) (2007) 897–904.
[17] N. Shaigan, W. Qu, T. Takeda, ECS Trans. 28 (32) (2010) 35–44.
[18] E. Deiss, F. Holzer, O. Haas, Electrochim. Acta 47 (25) (2002) 3995–4010.
[19] H. Song, X. Xu, F. Li, Acta Phys. Chim. Sin. 29 (9) (2013) 1961–1974.
[20] G. Bauer, V. Gravemeier, W.A. Wall, Int. J. Numer. Methods Eng. 86 (11) (2011) 1339–1359.
[21] W.A. Braff, C.R. Buie, ECS Trans. 33 (39) (2011) 179–190.
[22] W.A. Braff, M.Z. Bazant, C.R. Buie, Nat. Commun. 4 (2013).
[23] I.N. Stranski, L. Von Krastanow, Akad. Wigs. Lit. Mainz Abh. Math. -Naturwiss. Kl. 146 (1939) 797.
[24] S. Lucas, P. Moskovkin, Thin Solid Films 518 (18) (2010) 5355–5361.
[25] T.A. Witten, L.M. Sander, Phys. Rev. Lett. 47 (19) (1981) 1400.
[26] G. Kahanda, M. Tomkiewicz, J. Electrochem. Soc. 136 (5) (1989) 1497–1502.
[27] C.P. Chen, J. Jorné, J. Electrochem. Soc. 137 (7) (1990) 2047–2051.
[28] P. Pei, Z. Ma, K. Wang, X. Wang, M. Song, H. Xu, J. Power Sources 249 (2014) 13–20.
[29] Y. Ein-Eli, M. Auinat, D. Starosvetsky, J. Power Sources 114 (2003) 330–337.
[30] P. Pei, K. Wang, Z. Ma, Appl. Energy 128 (2014) 315–324.